FEBS Letters 584 (2010) 4351–4356

journal homepage: www.FEBSLetters.org

Solution structure of the carboxy-terminal Tudor domain from human Coilin

Riya Shanbhag, Arwa Kurabi, Jamie J. Kwan, Logan W. Donaldson *

Department of Biology, York University, Toronto, ON, Canada M3J 1P3

ARTICLE INFO

Article history:
Received 4 August 2010
Revised 15 September 2010
Accepted 22 September 2010
Available online 28 September 2010

Edited by Christian Griesinger

Keywords:
Cajal body
Splicing
Neuronal signaling
NMR

ABSTRACT

The Cajal body is a dynamic eukaryotic nuclear organelle that is known primarily as an organizational center for the assembly of snRNAs involved in transcript splicing. One of the most critical components of the Cajal body is the scaffolding protein, Coilin. Here, we demonstrate by NMR methods that the carboxy-terminal region contains a Tudor domain. The Tudor domain is atypical due to the presence of several unstructured loops, one greater than thirty amino acids in length. Tudor domains have been noted previously to bind DNA, RNA and modified amino acids. The absence of these sequence and structural signatures in the Coilin Tudor domain supporting these established functions suggests an alternative role.

1. Introduction

Coilin was initially discovered in sera from patients afflicted with autoimmune disease [1,2]. Its primary role is to serve as an organizational center in Cajal bodies – nuclear suborganelles 300–500 nm in diameter, that typically occur near histone gene clusters and the nucleolus [3]. In addition to Coilin, Cajal bodies are rich in snRNA, ribonucleoproteins, basal transcription factors and additional enzymes that perform critical post-transcriptional modifications such as 2′-O-methylation and pseudouridylation. Knockout mice for Coilin demonstrate reduced viability and fertility and fail to recruit several key proteins to the Cajal body, including snRNPs and the survival motor neuron (SMN) protein complex [4]. Coilin has also been observed to accumulate at damaged chromosomes during adenovirus and herpes simplex virus type 1 infections [5].

Human Coilin is a 576 aa. protein that can be loosely divided into three regions. The N-terminus is responsible for self-association leading to the characteristic fibrous pattern observed in Cajal bodies [6]. The only features that distinguish the interior 300 aa. are two nuclear localization signal sequences (NLS) and a region rich in arginine and glycine (RG-box). Symmetrical methylation of arginine in the RG-box recruits SMN through its Tudor domain [7]. Defects in SMN are responsible for spinal muscle atrophy disease, the second most common genetic cause of mortality in children after cystic fibrosis [8]. Our interest in Coilin lies in its partnership with AIDA-1 [9], a neuronal scaffolding protein that translocates from the postsynaptic complex to the nucleus in response to glutamate receptor stimulation [10]. A prior yeast two-hybrid interaction study revealed that an isoform of AIDA-1, composed primarily of two sterile alpha motif (SAM) domains and one phoshotyrosine binding (PTB) domain, interacts with the C-terminal region of Coilin [320–566].

Using conventional heteronuclear NMR methods, we have identified a folded domain in Coilin [460–576] and determined its solution structure to be an atypical Tudor domain bearing two large, unstructured loops. This structure provides a framework for understanding how protein interactions and post-translational modifications may contribute to the function of Coilin.

2. Materials and methods

2.1. Cloning and expression

A plasmid encoding a portion of human Coilin [320–576] was provided by Dr. Michael Hebert (Univ. Mississippi) and used to PCR amplify several shorter gene fragments flanked by *NdeI* and *XhoI* restriction sites for subsequent insertion into pET28a (Novagen). DNA sequencing revealed two discrepancies in all of the cloned Coilin genes as compared to the Genbank sequence for p80-Coilin (gi:4758024). Specifically, a 1508A>G change producing a K496E substitution and a 1633C>T silent change (A537A) were observed. A Coilin loop variant was synthesized by GenScript (Piscataway, NJ) and subcloned into pET28a. An alanine scan of two large loops in Coilin was achieved by direct synthesis of the mutant genes and subsequent insertion into the expression vector, pJExpress405 by

* Corresponding author. Address: Department of Biology, York University, 4700 Keele Street, Toronto, Ontario, Canada M3J 1P3. Fax: +1 416 736 5698.
E-mail address: logand@yorku.ca (L.W. Donaldson).

0014-5793/$36.00
doi:10.1016/j.febslet.2010.09.034

DNA2.0 (Menlo Park, CA). All cloned and directly synthesized genes were His_6 tagged to facilitate purification. Upon expression for 2–4 h in a standard M9 minimal medium containing 1 g/l ^{15}N NH_4Cl and 3 g/l ^{13}C-glucose as the sole nitrogen and carbon sources, the resulting proteins partitioned in *Esherichia coli* either exclusively as inclusion bodies, as part of the soluble fraction, or a combination of both. Cell pellets from inclusion bodies were resolubilized in 8 M guanidinium hydrochloride and cleared by centrifugation. Refolding was initiated by rapidly diluting the denatured protein solution into a 40-fold excess of 20 mM Tris–HCl pH 7.8, 0.3 M NaCl, which was followed by a conventional affinity purification for soluble proteins using Ni-NTA resin (Qiagen). Affinity-tags were cleaved with human thrombin (Sigma–Aldrich) as required and purified further by gel filtration chromatography (Sephacryl S–100, 16/60, GE Biosciences). Final buffer conditions for all protein studies, including NMR spectroscopy, were 20 mM Na-phosphate, pH 7.8, 0.15 M NaCl, 0.05% NaN_3, 10% D_2O.

2.2. CD spectroscopy

Far UV spectra of Coilin fragments were acquired with a Jasco J-810 instrument at a protein concentration of 20 μM in a buffer solution 5 mM Tris–HCl, pH 7.8, 50 mM NaCl. A rectangular cell with a 0.1 cm path length was used for all measurements. Spectra were recorded from 260 to 200 nm with a scan rate of 50 nm/min and a 1.0 nm bandwidth. A midpoint denaturation temperature (T_m) was determined by heating samples from 20 to 90 °C at 2 °C/min and monitoring ellipticity at 222 nm.

2.3. NMR measurements and structure determination

Chemical shift assignments on a uniformly ^{15}N, ^{13}C isotopically labeled sample of Coilin [460–576] at 0.6 mM were obtained using a conventional heteronuclear, triple-resonance strategy incorporating the backbone experiments: HNCACB, CBCA(CO)NH, HNCO, HNCACO H(C)(CO)NH, C(CO)NH, HB(CBCG)CD, the side chain experiments: H(C)(CO)NH, C(CO)NH, and the aromatic experiments: HB(CBCG)CD and HB(CBCGCD)CE. Distance restraints for structure calculations were obtained from a ^{15}N-edited NOESY (100 ms), and two ^{13}C-edited NOESYs (100 ms) centered on the aliphatic and aromatic regions. Backbone torsion angle restraints were predicted from chemical shifts using TALOS+ [11]. All experiments were acquired at 20 °C using a Varian NMRS 600 MHz spectrometer equipped with a Gen3 salt-tolerant cold probe. Datasets were processed with NMRPipe [12] and interpreted with a customized NMRView [13]. Structure calculations were performed with CYANA 2.1 [14] on a 100 CPU cluster sponsored by the Canadian computing consortium, SHARCNET, enhanced with virtualization software supplied by GridCentric Labs (Toronto, ON). Of 500 structures calculated, 25 were selected for further refinement sorted by CYANA target function. A refinement was performed using a customized simulated annealing script for XPLOR-NIH v2.26 that incorporated both a water refinement strategy [15] and a multidimensional torsion angle potential function [16]. The top 15 structures were assessed as a final ensemble with PROCHECK [17].

A relaxation study was performed by acquiring a series of ^{15}N-T_1 and ^{15}N-T_2 spectra at 600 MHz and temperatures of 20 °C and 25 °C with the following delays: T_1 – 10, 50, 90, 150, 210, 310, 410 ms; T_2 – 16.3, 32.6, 48.9, 65.2, 81.6, 97.9, 114.2 and 130.5 ms. The nLinLS module of NMRPipe was used to integrate and normalize resonances. The data were fit to a monoexponential function. Of the 50 resonances selected for analysis, a subset was chosen for a correlation time determination based on the criterion of having a T_1/T_2 ratio within one standard deviation of the average. A Mathematica script written by Dr. Pascal Mercier (Univ. Alberta) was used to determine a global correlation time from the T_1 and T_2 data.

2.4. Deposition of assignments and structure coordinates

Coordinates of the structural ensemble and restraint lists were deposited in the Protein Data Bank under accession code 2KDJ. Chemical shift assignments were deposited in the BMRB under accession code 16115.

3. Results and discussion

3.1. Protein fragment survey

Primary sequence searches performed with BLAST against the Conserved Domain Database (NCBI) and against the Protein Data Bank did not reveal any domains in Coilin [320–576]. In contrast to the primary structure analysis, a secondary structure analysis using PredictProtein [18] predicted several β-strands spanning the region K476-W554 suggesting that a domain could be present. Using this secondary structure signature as input for the SSEA method [19], one promising hit was the SH3 domain of Eps8 (PDB: 1AOJ) with a Z-score of 2.80. To assess the biological relevance of the secondary structure predictions, seven Coilin protein fragments were expressed and isotopically labeled with ^{15}N for analysis by NMR methods (Fig. 1). Four of the seven proteins were purified and determined to be monomeric after a final chromatography step using gel filtration. Using chemical shift dispersion as a guide, the ^{15}N-edited HSQC spectra of the four protein fragments suggested the presence of a folded domain within each of them. Ultimately, Coilin [460–576] was selected as the best candidate for a structural determination based upon the criteria of minimal length and maximum solubility.

3.2. Structural attributes

Statistics for the structural ensemble are presented in Table 1. As shown in Fig. 2a and b, the Coilin C-terminus contains a Tudor domain comprised of four characteristic β-strands and one short 3_{10} helix. Tudor domains are highly versatile ligand-binding modules that have been documented to interact with RNA, DNA, and methylated amino acids. Typical of a short motif, the hydrophobic core is characterized by only eight residues (Fig. 2c). A sequence analysis of Coilin homologs from seven representative species is presented in Fig. 2e.

From the structural ensemble, the most C-terminal structured amino acid in Coilin [460–576] was D559. When a gene fragment encoding Coilin [460–559] was expressed, the resulting inclusion bodies could not be refolded from denaturant. Consequently, we hypothesized that the region from 559 to 576 may contribute to the structural integrity of the Coilin Tudor domain. Some initial support for this hypothesis came from an inspection of a typical SH3 domain where an additional β-strand is found at an analogous position to aa. 561–564 in Coilin. However, we observed no backbone or side chain NOEs that would support a β-strand from 561 to 564 and no NOEs from the assigned methyl groups of I563 and I564 that would indicate a tight interaction with the Tudor domain.

The most striking attribute of the Coilin Tudor domain is the presence of two unstructured loops, β1β2 and β3β4, characterized by few chemical shift assignments presumably due to intermediate time scale conformational changes and its associated severe line broadening. The extent of the backbone chemical shift assignments made for the Coilin Tudor domain is illustrated in Fig. 2d. Despite its small size, 39 of the 117 amide resonances in Coilin [470–576] were unobservable or unassignable, with the majority of those residing in the unstructured loops. For the amides that were present, we performed a ^{15}N T_1/T_2 relaxation analysis and determined a correlation time of 10.6 ns and 8.9 ns at 20 °C and 25 °C, respectively.

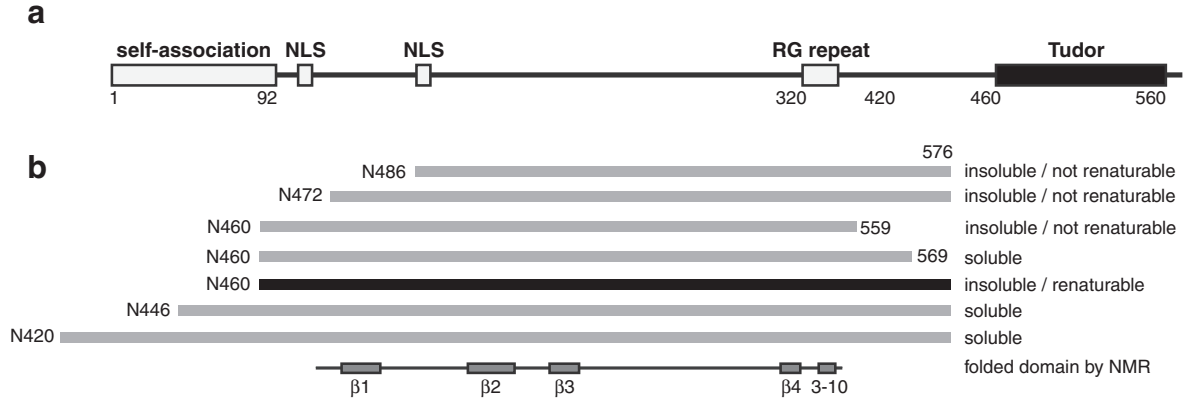

Fig. 1. Domain organization of Coilin. (a) The Tudor domain described in this study is located at the extreme C-terminus. Sequences previously associated with a biological function include a self-association region of unknown structure, two nuclear localization sequences (NLS) and an arginine–glycine (RG) repeat region known to be a binding site for the survival-motor-neuron (SMN) Tudor domain. (b) N- and C-terminal fragments encompassing the Tudor domain were observed to express in both inclusion bodies and the soluble fractions of *E. coli*. The fragment selected for NMR studies, Coilin [460–576] was expressed in inclusion bodies, but could be quantitatively refolded from denaturant.

Table 1
Restraints and statistics for the ensemble of 15 structures.

NOE restraints	
Total	584
Intraresidue ($\|i-j\|=0$)	272
Sequential ($\|i-j\|=1$)	177
Medium range ($1<\|i-j\|<5$)	30
Long range ($\|i-j\|\geqslant 5$)	105
Additional restraints	
Hydrogen bond distance restraint pairs (H–O, HN–O)	11
φ/Ψ torsion angle restraint pairs[a]	23
Violations	
RMS bond distances (Å)	0.0063 ± 0.0003
RMS angles (°)	0.6118 ± 0.0259
RMS improper angles (°)	0.8984 ± 0.0527
RMS dihedral angles (°)	0.0000 ± 0.0000
RMS NOE violations >0.3 (Å)	1.2667 ± 1.1629
RMS NOE violations >0.1 (Å)	16.6667 ± 3.1997
Ramachandran analysis[b]	
Most favored regions	84.1%
Additional allowed regions	14.0%
Generously allowed regions	1.0%
Disallowed regions	0.9%
RMSD to average coordinates	
Tudor domain secondary structures[c]	
Backbone atoms (Å)	0.58 ± 0.11 Å
Heavy atoms (Å)	1.59 ± 0.29 Å

[a] Predicted by TALOS+ (Shen et al., 2009).
[b] Assessed by PROCHECK-NMR (Laskowski et al., 1996) for residues 474–561.
[c] Residues 476–479, 496–500, 510–514, 549–552.

These values are greater than the 7.7 ns at 25 °C observed for the *Drosophila* Pcl Tudor domain [20]; however, it must be considered in hydrodynamic terms that the loops of the Coilin Tudor could result in a much larger Stokes radius than the relatively compact Pcl Tudor domain. Supporting this conclusion, analytical gel filtration and glutaraldehyde crosslinking both demonstrated that the Coilin Tudor domain is monomeric in solution.

We performed a survey of Tudor domain structures from the Protein Data Bank. Of the 30 unique structures we curated, eight were observed to bind methylated amino acids, five were observed to bind proteins or peptides, and two were observed to bind nucleic acids. The remaining 15 structures in the dataset have no ascribed function. The full table is available as Supplementary data.

The ability of the Coilin Tudor domain to interact with methylated amino acids was assayed by titrating solutions of monomethyl-lysine, trimethyl-lysine and dimethyl-arginine into ^{15}N-labeled Coilin [460–576]. No amide chemical shift changes were observed at up to a 20-fold excess of titrant suggesting that the Coilin Tudor domain does not bind methylated amino acids. Supporting these observations, an inspection of the Coilin Tudor domain structure did not identify the characteristic aromatic cage found in family members such as 53BP1 [21] that are known to bind methylated histones (Fig. 3).

The lack of a basic surface patch on the Coilin Tudor domain suggests that it does not bind nucleic acids. Furthermore, the absence of a hydrophobic protein/peptide binding site analogous to the Cul7 CPH domain suggests that this binding mode is not utilized by Coilin.

While the total amount of Coilin remains constant throughout the cell cycle, the phosphorylation state varies greatly, and in turn, affects its cellular localization, self-assembly, and interactions with other proteins. The 17 aa. β1β2 loop contains a serine (S389), that upon phosphorylation, alters the relative amounts of SmB′ (an RNA binding protein) and SMN that is bound to Coilin [22]. By occurring in a dynamic, poorly structured state, the β1β2 loop is highly accessible to a Ser/Thr kinase and is poised to communicate structural and dynamic changes in response to phosphorylation [23]. Since the Tudor domain and the RG-box to which SMN binds are separated by approximately 100 aa., Coilin, like many signaling scaffolding proteins, may be regulated by a combination of intra- and intermolecular interactions.

At 35 aa. in length, the β3β4 loop is predominantly unstructured. We demonstrated the dispensability of the β1β2 and β3β4 loops to the Tudor domain by designing and expressing two variants that had one or both loops replaced with a canonical β-turn motif bearing the sequence, DPxG. The β1β2 singly loopless variant was expressed and purified as a soluble glutathione S-transferase (GST)-fusion protein but upon cleavage from the GST carrier, the Coilin variant was aggregated by analytical gel filtration and NMR methods. In contrast, the doubly loopless β1β2/β3β4 variant was soluble, although sparingly to a maximum of 0.1 mM. A ^{15}N-edited HSQC spectrum of the doubly loopless variant was consistent with a folded protein fragment; however, many qualitative differences in the spectra were apparent suggesting concomitant structural differences. To assess these structural differences in detail, we attempted to assign the loopless β1β2/β3β4 variant but were ultimately precluded due to low solubility <0.1 mM of the sample. From a parallel circular dichroism (CD) spectroscopic study of Coilin [460–569] and the β1β2/β3β4 loopless variant, we obtained thermal denaturation midpoints (T_m) of 62 and 56 °C,

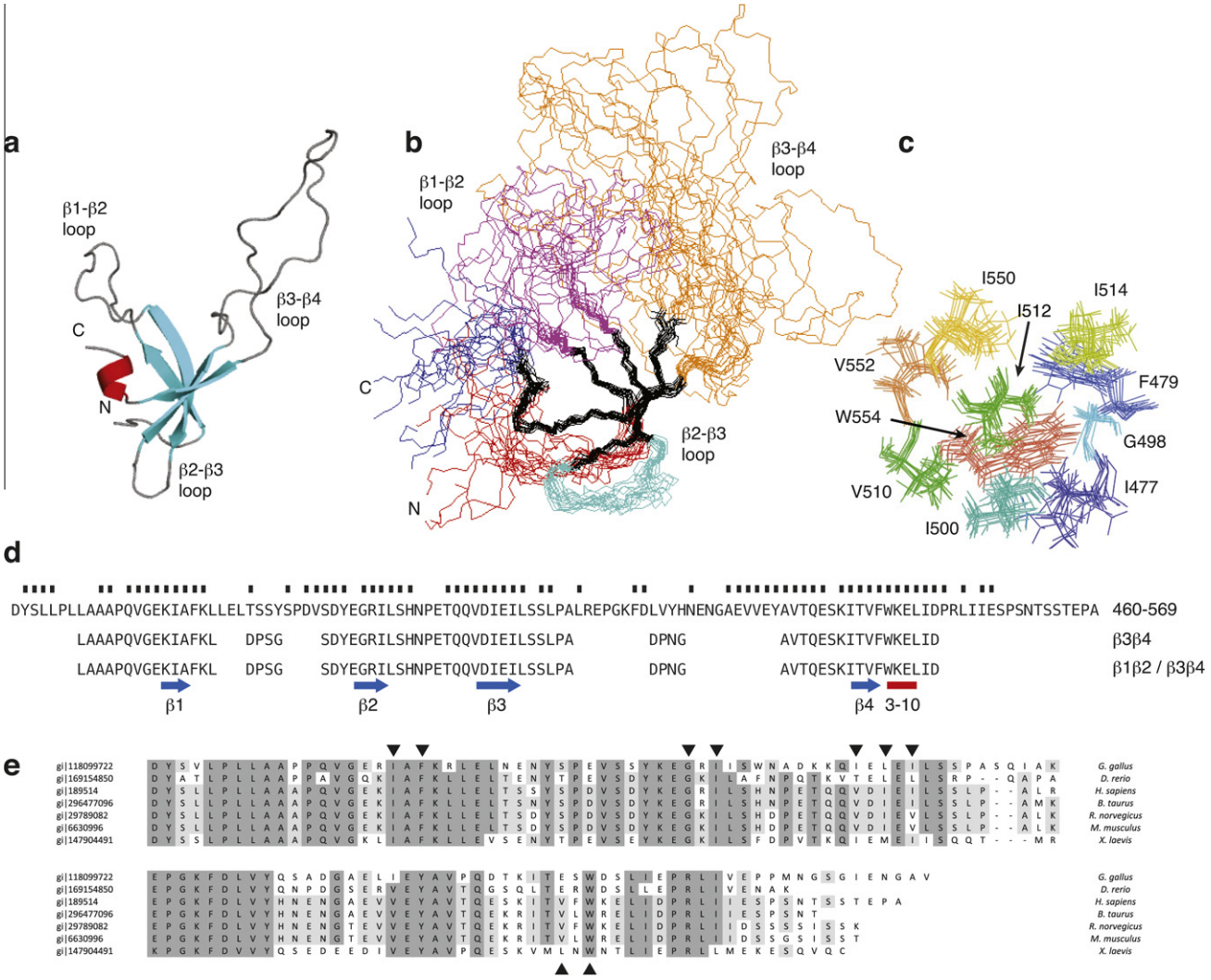

Fig. 2. The NMR structure of Coilin [460–576]. (a) Ribbon representation highlighting the four β-strands and a short 3_{10} helix that is found in many SH3 domains. (b and c) Superposition of 20 lowest energy NMR structures. (d) A C-terminally truncated protein fragment, Coilin [460–569] was soluble and folded as well as a synthetic, loopless Coilin [460–569] protein fragment that had the β23 and β34 loops substituted with a β-turn. Rectangles above the sequence denote amino acids for which an amide backbone assignment was determined. (e) A sequence alignment of the Coilin Tudor domain from seven representative species. Triangles denote residues in the hydrophobic core.

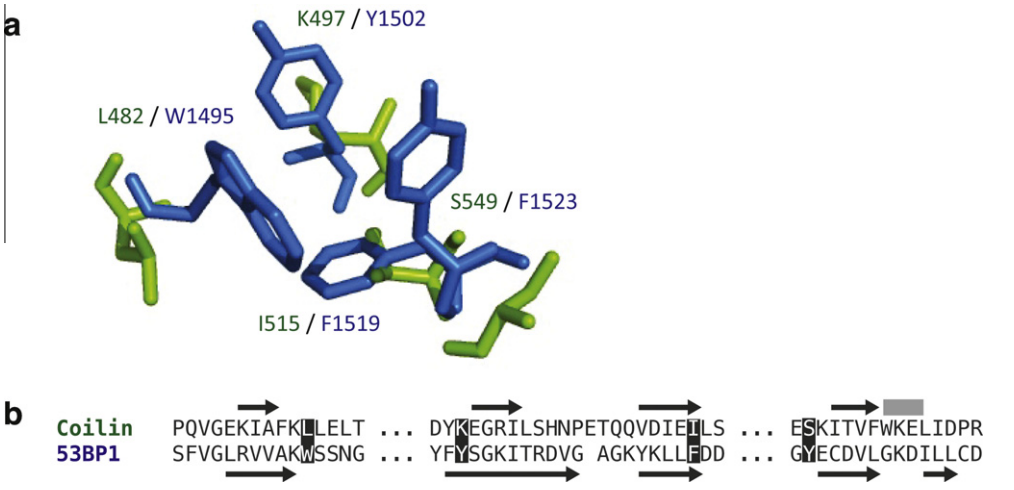

Fig. 3. The Coilin Tudor domain does not demonstrate an aromatic cage that is characteristic of family members that bind methylated amino acids. (a) The Coilin Tudor domain structure was aligned with the first Tudor domain of 53BP1 (PDB: 2IG0), known to bind dimethylated arginine. The aromatic cage of 53BP1 (blue) is shown along with the residues at an analogous position in Coilin (green). (b) Sequence alignment and secondary structure of 53BP1 and Coilin. The aromatic cage positions are indicated.

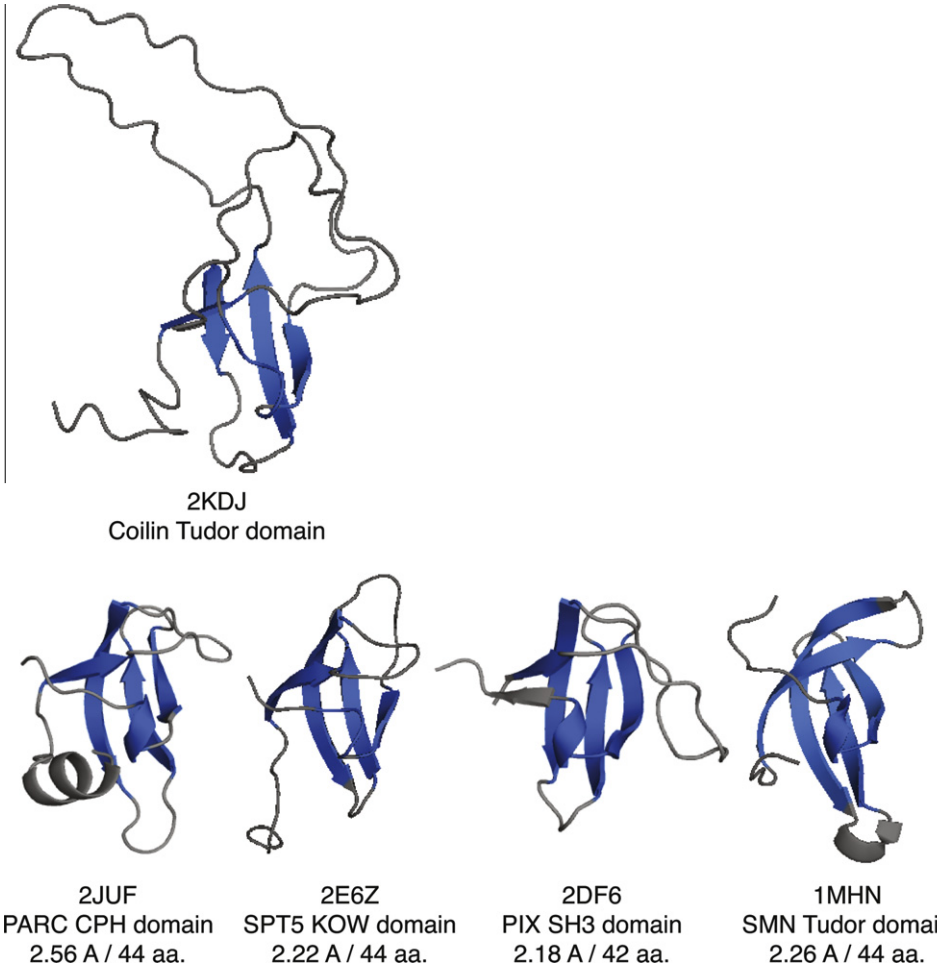

Fig. 4. The Coilin Tudor domain and a representative superfamily of structurally related domains.

respectively. Taken together, the NMR and CD studies suggest that the loops are indeed dispensable and the N- and C-terminal boundaries of the loopless variants are consistent with the structural boundaries of the Tudor domain.

The deletion analysis of the β1β2 and β3β4 loops was augmented by an alanine scan. Substitution of a 484-AAAAA-488 mutant essentially replacing most of the β1β2 loop had a minor effect on the structural as judged by comparison of ^{15}N-edited HSQC spectra with a wild type protein fragment. The β3β4 loop was successively scanned with three mutants: 523-AAAAA-527, 528-AAAAA-532, and 533-AAAAA-537. From this analysis, residues 528–537 of the β3β4 loop could be substituted without causing any major structural changes. In contrast to the observations described for the loopless mutant, the 523-AAAAA-527 mutant demonstrated the spectrum of an aggregated, misfolded protein. While this result was unexpected, the body of mutational data suggests that the β1β2 and β3β4 loops do not contribute substantially to the structure of the Coilin Tudor domain.

4. Conclusions

Through a combination of bioinformatics, deletion analysis and NMR spectroscopy, we have determined that the Coilin C-terminus contains a Tudor domain. This diverse fold bears many similarities to KOW [24], CPH [25] and SH3 domains [26], of which some are shown in Fig. 4 for comparison. Inspection of the Coilin Tudor domain surface revealed no obvious signature of amino acids that would support binding to methylated amino acids, proteins or nucleic acids leading to the possibility that the Tudor domain fulfills a novel function, perhaps by supplying a binding site in the β3β4 loop for a protein partner or by serving as a substrate for phosphorylation.

Acknowledgement

We are grateful to Dr. Michael Hebert for many valuable conversations regarding the biology of Coilin and sharing unpublished data. This work was supported by Natural Sciences and Engineering Research Council (NSERC) Discovery Grant 2389346 to L.W.D.

Appendix A. Supplementary data

Supplementary data associated with this article can be found, in the online version, at doi:10.1016/j.febslet.2010.09.034.

References

[1] Andrade, L.E., Chan, E.K., Raska, I., Peebles, C.L., Roos, G. and Tan, E.M. (1991) Human autoantibody to a novel protein of the nuclear coiled body: immunological characterization and cDNA cloning of p80-coilin. J. Exp. Med. 173, 1407–1419.
[2] Raska, I., Andrade, L.E., Ochs, R.L., Chan, E.K., Chang, C.M., Roos, G. and Tan, E.M. (1991) Immunological and ultrastructural studies of the nuclear coiled body with autoimmune antibodies. Exp. Cell Res. 195, 27–37.

[3] Morris, G.E. (2008) The Cajal body. Biochim. Biophys. Acta 1783, 2108–2115.
[4] Walker, M.P., Tian, L. and Matera, A.G. (2009) Reduced viability, fertility and fecundity in mice lacking the cajal body marker protein, coilin. PLoS ONE 4, e6171.
[5] Morency, E., Sabra, M., Catez, F., Texier, P. and Lomonte, P. (2007) A novel cell response triggered by interphase centromere structural instability. J. Cell Biol. 177, 757–768.
[6] Hebert, M.D. and Matera, A.G. (2000) Self-association of Coilin reveals a common theme in nuclear body localization. Mol. Biol. Cell 11, 4159–4171.
[7] Hebert, M.D., Szymczyk, P.W., Shpargel, K.B. and Matera, A.G. (2001) Coilin forms the bridge between Cajal bodies and SMN, the spinal muscular atrophy protein. Genes Dev. 15, 2720–2729.
[8] Lunn, M.R. and Wang, C.H. (2008) Spinal muscular atrophy. Lancet 371, 2120–2133.
[9] Xu, H. and Hebert, M.D. (2005) A novel EB-1/AIDA-1 isoform, AIDA-1c, interacts with the Cajal body protein coilin. BMC Cell Biol. 6, 23.
[10] Jordan, B.A., Fernholz, B.D., Khatri, L. and Ziff, E.B. (2007) Activity-dependent AIDA-1 nuclear signaling regulates nucleolar numbers and protein synthesis in neurons. Nat. Neurosci. 10, 427–435.
[11] Shen, Y., Delaglio, F., Cornilescu, G. and BAx, A. (2009) TALOS+: a hybrid method for predicting protein backbone torsion angles from NMR chemical shifts. J. Biomol. NMR 44, 213–223.
[12] Delaglio, F., Grzesiek, S., Vuister, G.W., Zhu, G., Pfeifer, J. and Bax, A. (1995) NMRPipe: a multidimensional spectral processing system based on UNIX pipes. J. Biomol. NMR 6, 277–293.
[13] Johson, B.A. and Blevins, R.A. (1994) NMRView: a computer program for the visualization and analysis of NMR data. J. Biomol. NMR 4, 603–614.
[14] Güntert, P., Mumenthaler, C. and Wüthrich, K. (1997) Torsion angle dynamics for NMR structure calculation with the new program DYANA. J. Mol. Biol. 273, 283–298.
[15] Linge, J.P., Williams, M.A., Spronk, C.A.E.M., Bonvin, A.M.J.J. and Nilges, M. (2003) Refinement of protein structures in explicit solvent. Proteins 50, 496–506.
[16] Kuszewski, J. and Clore, G.M. (2000) Sources of and solutions to problems in the refinement of protein NMR structures against torsion angle potentials of mean force. J. Magn. Reson. 146, 249–254.
[17] Laskowski, R.A., Rullmann, J.A., MacArthur, M.W., Kaptein, R. and Thornton, J.M. (1996) AQUA and PROCHECK-NMR: programs for checking the quality of protein structures solved by NMR. J. Biolmol. NMR 8, 477–486.
[18] Rost, B. and Liu, J. (2003) The PredictProtein server. Nucleic Acids Res. 31, 3300–3304.
[19] Fontana, P., Bindewald, E., Toppo, S., Velasco, R., Valle, G. and Tosatto, S.C.E. (2005) The SSEA server for protein secondary structure alignment. Bioinformatics 21, 393–395.
[20] Friberg, A., Oddone, A., Klymenko, T., Muller, J. and Sattler, M. (2010) Structure of an atypical Tudor domain in the *Drosophila* Polycomblike protein. Protein Sci. (Epub 07/14/2010).
[21] Botuyan, M.V., Lee, J., Ward, I.M., Kim, J.E., Thompson, J.R., Chen, J. and Mer, G. (2006) Structural basis for the methylation state-specific recognition of histone H4-K20 by 53BP1 and Crb2 in DNA repair. Cell 127, 1361–1373.
[22] Toyota, C.G., Davis, M.D., Cosman, A.M. and Hebert, M.D. (2009) Coilin phosphorylation mediates interaction with SMN and SmB′. Chromosoma 119, 1–11.
[23] Iakoucheva, L.M., Radiivojac, P., Brown, C.J., O'Connor, T.R., Sikes, J.G., Obradovic, Z. and Dunker, A.K. (2004) The importance of intrinsic disorder for protein phosphorylation. Nucleic Acids Res. 32, 1037–1049.
[24] Kyrpides, N.C., Woese, C.R. and Ouzounis, C.A. (1996) KOW: a novel motif linking a bacterial transcription factor with ribosomal proteins1. Trends Biochem. Sci. 21, 425–426.
[25] Kaustov, L., Lukin, J., Lemak, A., Duan, S., Ho, M., Doherty, R., Penn, L.Z. and Arrowsmith, C.H. (2007) The conserved CPH domains of Cul7 and PARC are protein-protein interaction modules that bind the tetramerization domain of p53. J. Biol. Chem. 282, 11300–11307.
[26] Hoelz, A., Janz, J.M., Lawrie, S.D., Corwin, B., Lee, A. and Sakmar, T.P. (2006) Crystal structure of the SH3 domain of betaPIX in complex with a high affinity peptide from PAK2. J. Mol. Biol. 358, 509–522.